**Marquette University**
## e-Publications@Marquette

Biomedical Engineering Faculty Research and Publications

Biomedical Engineering, Department of

1-31-2015

# Kinematic Foot Types in Youth with Equinovarus Secondary to Hemiplegia

Joseph Krzak
*Shriners Hospitals for Children*

Daniel M. Corcos
*University of Illinois at Chicago*

Diane L. Damiano
*National Institutes of Health*

Adam Graf
*Shriners Hospitals for Children*

Donald Hedeker
*University of Chicago*

**See next page for additional authors**

**Authors**

Joseph Krzak, Daniel M. Corcos, Diane L. Damiano, Adam Graf, Donald Hedeker, Peter A. Smith, and Gerald F. Harris

# Kinematic Foot Types in Youth with Equinovarus Secondary to Hemiplegia

## Joseph J. Krzak

*Midwestern University, Physical Therapy Program,*
*College of Health Sciences,*
*Downers Grove, IL*
*Shriners Hospitals for Children®-Chicago,*
*Chicago, IL*

## Daniel M. Corcos

*Northwestern University Feinberg School of Medicine,*
*Department of Physical Therapy and Human Movement Sciences,*
*Chicago, IL*

## Diane L. Damiano

*National Institutes of Health,*
*Functional & Applied Biomechanics Section,*
*Bethesda, MD*

## Adam Graf

*Shriners Hospitals for Children®-Chicago,*
*Chicago, IL*

# Donald Hedeker
*University of Chicago, Department of Public Health Sciences, Chicago, IL*

# Peter A. Smith
*Shriners Hospitals for Children®-Chicago,*
*RUSH University Medical Center,*
*Department of Orthopaedic Surgery, College of Medicine, Chicago, IL*

# Gerald F. Harris
*Shriners Hospitals for Children®-Chicago, Chicago, IL*
*Orthopaedic & Rehabilitation Engineering Center (OREC), Marquette University/Medical College of Wisconsin, Milwaukee, WI*

## Abstract

**Background:** Elevated kinematic variability of the foot and ankle segments exists during gait among individuals with equinovarus secondary to hemiplegic cerebral palsy (CP). Clinicians have previously addressed such variability by developing classification schemes to identify subgroups of individuals based on their kinematics.

**Objective:** To identify kinematic subgroups among youth with equinovarus secondary to CP using 3-dimensional multi-segment foot and ankle kinematics during locomotion as inputs for principal component analysis (PCA), and *K*-means cluster analysis.

**Methods:** In a single assessment session, multi-segment foot and ankle kinematics using the Milwaukee Foot Model (MFM) were collected in 24 children/adolescents with equinovarus and 20 typically developing children/adolescents.

**Results:** PCA was used as a data reduction technique on 40 variables. *K*-means cluster analysis was performed on the first six principal components (PCs) which accounted for 92% of the variance of the dataset. The PCs described the location and plane of involvement in the foot and ankle. Five distinct kinematic subgroups were identified using *K*-means clustering. Participants with equinovarus presented with variable involvement ranging from primary hindfoot or forefoot deviations to deformtiy that included both segments in multiple planes.

**Conclusion:** This study provides further evidence of the variability in foot characteristics associated with equinovarus secondary to hemiplegic CP.

These findings would not have been detected using a single segment foot model. The identification of multiple kinematic subgroups with unique foot and ankle characteristics has the potential to improve treatment since similar patients within a subgroup are likely to benefit from the same intervention(s).

**Keywords:** Cerebral palsy, Equinovarus, Gait, Multi-segmental foot modeling

# 1. Introduction

Equinus and varus, often in combination, are the most common foot and ankle deformities in children with hemiplegic cerebral palsy (CP).[1] Static or dynamic soft tissue imbalance results in combinations of segmental deformities including hindfoot equinus and inversion, midfoot cavus, as well as, forefoot supination and adduction. Beyond atypical foot position interfering with stance phase stability and swing phase clearance, these deformities are associated with gait deviations at more proximal segments, increased mechanical work, and increased energy expenditure in children with CP.[2–4]

Although equinovarus is a specific deformity commonly recognized in children with hemiplegic CP, individual segmental contributions are significantly variable. Such variability has resulted in inconsistent gait kinematics, multiple combinations of corrective surgical techniques, and fluctuating post-operative success rates of 67–82%.[5–9] Post-operative success can further decline when non-systematic data interpretation methods are used for treatment planning. Efforts to facilitate treatment planning and improve post-operative outcomes in the presence of variable gait patterns used whole-body kinematic classification schemes that identified clinical subgroups. For example, Winters and colleagues[10] proposed a lower limb classification that differentiated children with hemiplegic CP into one of the four subgroups based on affected joints. Such methods were intended to help standardize data interpretation and direct treatment since similar patients within a subgroup will likely benefit from the same intervention(s).

Differentiating individuals with equinovarus into kinematic subgroups becomes plausible when considering the potential neuromuscular contributor(s) to the deformity. Electromyography (EMG) studies have demonstrated that varus deformity in children with hemiplegic CP most commonly results from non-phasic firing patterns of the anterior or posterior tibialis, acting either independently or in

combination.[11] The ankle plantar flexors, particularly the soleus, are also potential contributors to equinovarus as they act as subtalar invertors due to a medial insertion of the Achilles tendon on the calcaneus.[12] Therefore, influences from the anterior tibialis, posterior tibialis, combined anterior/posterior tibialis, and plantar flexors can impact segmental characteristics of the foot and ankle resulting in up to four kinematic subgroups of equinovarus.

Two limitations of applying the methods used by Winters to identify kinematic subgroups of equinovarus are that the whole-body kinematic model used lacks the complexity to detect subtle foot and ankle deformities and the previous classifications were not systematically determined using the most current statistical methods. Multi-segment foot and ankle modeling using the Milwaukee Foot Model (MFM) is an option to measure 3-D kinematics during locomotion.[13] The MFM has been used to quantify multi-segment kinematics in children with equinovarus.[14] It uses radiographic skeletal indexing to mathematically orient the surface marker-based local coordinate axes to the underlying skeletal anatomy which makes it ideal for quantifying the kinematics of small foot segments that lack reliable bony landmarks.

Recently, systematic approaches to developing gait classifications have included principal component analysis (PCA) and cluster analysis. PCA has been employed to identify the most salient variables from large datasets while minimizing loss of valuable information.[15,16] In a sample of 20 children with diplegic CP and 20 typically developing (TD) children, Carriero and colleagues[15] used PCA to reduce 26 kinematic variables and participant age to three principal components which accounted for 61% of the variance in the original dataset. Once a dataset is reduced, cluster analysis can then be performed on the principal components to identify subgroups of similar individuals. *K*-means clustering is one of the multiple clustering techniques and has previously been used as an effective method to identify subgroups of crouch gait severity among children with bilateral CP.[17]

The purpose of the current study was to identify clinically relevant subgroups among a sample of TD children and children with equinovarus due to hemiplegic CP by using multi-segment foot

kinematics as inputs for PCA and *K*-means cluster analysis. We anticipated that each subgroup would present with unique kinematic characteristics of equinovarus including varying involvement of specific segment(s), plane(s), timing, and the joint excursions associated with the deformity.

## 2. Methods

### 2.1. Participants

Twenty four children/adolescents with hemiplegic CP (13 males, 11 females, average age: 12.0 ± 4.1 years, 13 right-sided, 11 left-sided) and a group of 20 TD children/adolescents (11 males, 9 females, average age: 11.8 ± 2.7 years) were included. All participants with CP had unilateral equinovarus foot deformity as determined by their treating physician and were recruited as a part of a diagnostic gait analysis with a plan for possible surgical correction consisting of musculotendinous lengthenings and/or transfers. Participants had no prior history of orthopedic surgery for equinovarus and had not received botulinum toxin injections within 1 year prior to evaluation. Individuals were excluded if they had cognitive or behavioral impairments that interfered with their ability to follow basic commands necessary to participate in gait analysis and a standing weight-bearing X-ray series. Participants were also excluded if the treating surgeon determined that the deformity was rigid enough to indicate osteotomies or joint procedures for surgical correction. Informed consent was provided from the participants' legal guardians and, when appropriate, assent/consent was obtained from the participants as approved by an institutional review board.

### 2.2. Instrumentation

Participants underwent quantitative gait analysis using the MFM.[13] Nine passive 9 mm reflective markers were placed on the tibia, calcaneus, and forefoot. Marker trajectories were collected at 120 Hz using a 14-MX camera 3-D motion analysis system and Vicon Nexus (version 1.8.4) software (VICON, Oxford, UK). The kinematic data were processed and calculated using a custom program written in Matlab (Mathworks®, Natick, MA, USA).

## 2.3. Experimental protocol

A static standing trial was collected with the participant standing on a cardboard sheet where a foot tracing was made. This tracing was later used to ensure that the same standing alignment was achieved during the radiographs. Participants were instructed to walk "at a comfortable walking speed" down a 30 m walkway. Between 10 and 15 trials were collected, and three representative trials were chosen for analysis. Twelve of these children performed a total of 20–30 trials as they participated in an additional experiment.[14]

Following gait data collection, a series of weight-bearing radiographs of the foot were taken. Anterior–posterior, lateral, and a modified hindfoot coronal alignment view were captured while standing on the foot tracing created during the static standing trial.[18] All radiographic measurements for skeletal indexing were obtained by the same author (JK).

## 2.4. Principal component analysis

The input data matrix of the PCA consisted of 38 multi-segment foot and ankle kinematic variables, walking speed, and age at the time of the preoperative evaluation. The kinematic variables were chosen via clinical consensus based on their ability to identify specific segment(s), plane(s), timing, and the relevant joint excursions associated with the deformity. These included hindfoot and forefoot peak motion, total ROM, and mean position throughout the gait cycle. Descriptive statistics of the 40 variables were computed for initial mean comparisons between children with CP and the TD children using Cohen's *d* effect size where the difference between the group means was divided by the pooled standard deviation.[19] Each variable was then normalized by subtracting the mean and dividing by the standard deviation across the entire sample. The PCs were derived from the correlation matrix of the normalized dataset using a Varimax rotation in IBM SPSS Statistics 20 (Chicago, IL). This resulted in 40 initial PCs. Specific criteria to retain variables and PCs have been established and were implemented to ensure that the variables were distinct measures of one specific PC. The criteria used for PC retention included: (1) an eigenvalue of ≥1.00,[20] (2) components located to the left of an 'elbow'

on the scree plot containing the eigenvalues across all PCs,[21] (3) retaining the minimum number of components such that the cumulative percent of variance accounted for was ≥80%.[22,23] Variables were retained in a particular component if: (1) at least 50% of the variance of the normalized variable was accounted for by the retained PCs ($h^2 \geq 0.50$), (2) the variable had a weighting score of ≥0.40 or ≤−0.40 on a PC, and (3) the variable demonstrated a simple structure (i.e. the weighting score of the particular variable was not ≥0.40 or ≤−0.40 on more than one PC.[24] If a variable(s) did not meet the retention criteria, it was removed and PCA was repeated using the remaining variables until all retention criteria were met. To determine if the final dataset was suitable for PCA, Bartlett's test of sphericity was performed.[25] To determine if the sampling was adequate for analysis, the Kaiser–Meyer–Olkin (KMO) test was also performed.[26] Once the final model was determined, individual PC scores were derived for each participant across all retained PCs for the subsequent cluster analysis using the following equation:PC score$_{ij} = \Sigma_k \bar{X}_{ik} a_{jk}$

The PC scores of the $i$th person and $j$th PC were calculated as the weighted sum of the kinematic variables retained within that particular PC. $\bar{X}_{ik}$ is original variable value averaged over three walking trials for the $k$th kinematic measure, and $a_{kj}$ is a matrix of weighting score coefficients converting the $k$ dimensional vector of kinematic measures into a six dimensional vector of PCs.

## 2.5. Cluster analysis

An initial hierarchical cluster analysis using squared Euclidian distances and Ward's method was performed on the standardized PC scores for all participants.[27,28] This was done to define the appropriate number of a priori clusters to be used in the $K$-means cluster analysis. Individual PC scores were standardized into $z$-scores to allow all PC scores to have equal influence on the initial cluster center locations in the $K$-means analysis. The optimal number of clusters to be used in the $K$-means analysis was determined by calculating the agglomeration distance coefficients across stages as additional cases from 1 to 44 were merged into the clusters. A scree diagram of the distance coefficients across stages was then used to identify the stage where the first significant change occurred in the coefficients as

additional cases were added to the clusters. The identified stage was subtracted from the total number of subjects ($n = 44$) to determine the appropriate number of clusters to be used in the *K*-means analysis. Subgroup membership via *K*-means analysis was then determined using a clustering algorithm that categorizes individuals based on the proximity to means, thus maximizing similarities within a subgroup and the differences among the subgroups.

Once subgroup membership was assigned using *K*-means cluster analysis, one-way analyses of variance (ANOVA) were performed to determine the effect of subgroup membership on PC scores. Where a main effect of membership was identified, post hoc, two-tailed, Dunnett's tests were performed to further analyze the pair-wise comparisons to a subgroup identified as the Control Group. The level of statistical significance was set at 0.05.

# 3. Results

Table 1 shows the means, standard deviations (SD), and ranges of the 40 chosen variables included in the initial PCA for children with CP and TD children. Effect sizes between the two groups demonstrated expected differences in walking speed and many of the kinematic parameters consistent with equinovarus deformity. Specifically, participants with CP walked slower and presented with a more plantar flexed and inverted hindfoot relative to the tibia, as well as, a forefoot in greater dorsiflexion and adduction relative to the hindfoot.

**Table 1.** Means, standard deviations (SD), and ranges of the 40 variables used in the initial iteration of the principal component analysis for children with hemiplegic cerebral palsy and typically developing children.

| Variables | CP | | | | Typically developing children | | | | Effect size |
|---|---|---|---|---|---|---|---|---|---|
| | Average | SD | Range | | Average | SD | Range | | |
| | | | Min | Max | | | Min | Max | |
| Age | 12.0 | 4.1 | 5.7 | 19.7 | 11.8 | 2.7 | 6.1 | 17.5 | 0.0 |
| Walking speed | 0.9 | 0.2 | 0.5 | 1.2 | 1.2 | 0.2 | 0.8 | 1.4 | 1.6 |
| Sagittal plane kinematics | | | | | | | | | |
| Sagittal hindfoot position at IC | 5.3 | 11.6 | −12.5 | 27.9 | 13.0 | 10.0 | −5.7 | 41.0 | 0.7 |
| Peak hindfoot dorsiflexion during stance | 12.3 | 13.3 | −11.7 | 34.5 | 27.6 | 9.9 | 6.1 | 46.6 | 1.3 |

| Variables | CP | | | | Typically developing children | | | | Effect size |
|---|---|---|---|---|---|---|---|---|---|
| | Average | SD | Range | | Average | SD | Range | | |
| | | | Min | Max | | | Min | Max | |
| Peak hindfoot plantarflexion during stance | −2.8 | 15.7 | −31.6 | 27.8 | 9.6 | 10.2 | −12.3 | 37.2 | 0.9 |
| Peak hindfoot dorsiflexion during swing | 7.5 | 12.7 | −13.6 | 35.5 | 23.9 | 9.8 | 3.3 | 46.5 | 1.5 |
| Peak hindfoot plantarflexion during swing | −4.0 | 15.5 | −34.2 | 28.3 | 9.8 | 10.0 | −5.8 | 38.9 | 1.1 |
| Sagittal hindfoot ROM during stance phase | 15.1 | 5.8 | 4.7 | 26.6 | 18.0 | 5.2 | 9.4 | 29.7 | 0.5 |
| Sagittal hindfoot ROM during swing phase | 11.5 | 5.7 | 3.6 | 22.9 | 14.1 | 4.9 | 4.6 | 22.2 | 0.5 |
| Sagittal hindfoot ROM throughout GC | 16.7 | 6.2 | 4.7 | 29.2 | 18.9 | 5.3 | 9.4 | 29.9 | 0.4 |
| Average sagittal hindfoot position during stance | 6.8 | 12.6 | −17.6 | 28.1 | 20.6 | 9.2 | 0.5 | 42.4 | 1.3 |
| Average sagittal hindfoot position during swing | 2.7 | 13.4 | −21.4 | 30.3 | 19.7 | 9.5 | 0.9 | 44.6 | 1.5 |
| Sagittal forefoot position at IC | −30.1 | 16.5 | −50.8 | 11.7 | −35.7 | 13.4 | −54.3 | −3.1 | 0.4 |
| Peak forefoot dorsiflexion throughout GC | −13.7 | 14.7 | −39.3 | 17.6 | −29.4 | 13.7 | −50.0 | 3.5 | 1.1 |
| Peak forefoot plantarflexion throughout GC | −32.8 | 15.5 | −52.8 | 3.4 | −40.3 | 14.1 | −61.2 | −6.8 | 0.5 |
| Sagittal forefoot ROM during stance | 16.4 | 7.0 | 6.2 | 29.6 | 9.7 | 2.2 | 6.9 | 15.1 | 1.3 |
| Sagittal forefoot ROM during swing | 15.1 | 7.8 | 3.4 | 31.5 | 6.6 | 3.1 | 2.5 | 16.6 | 1.4 |
| Sagittal forefoot ROM throughout GC | 19.1 | 7.0 | 8.1 | 31.5 | 12.2 | 7.3 | 6.9 | 40.4 | 1.0 |
| Average sagittal forefoot position throughout GC | −23.2 | 14.9 | −45.5 | 11.6 | −33.3 | 14.9 | −57.1 | −2.4 | 0.7 |
| Coronal plane kinematics | | | | | | | | | |
| Coronal hindfoot position at IC | −16.0 | 10.0 | −39.3 | 5.1 | −4.9 | 11.4 | −23.9 | 8.4 | 1.1 |
| Peak hindfoot eversion throughout GC | −8.9 | 11.4 | −37.8 | 21.7 | 6.6 | 9.3 | −10.4 | 19.4 | 1.5 |
| Peak hindfoot inversion throughout GC | −21.7 | 11.8 | −47.7 | 1.4 | −7.8 | 10.8 | −24.5 | 4.8 | 1.3 |
| Coronal hindfoot ROM during stance | 10.9 | 6.6 | 2.1 | 28.4 | 11.3 | 6.9 | 3.7 | 27.0 | 0.1 |
| Coronal hindfoot ROM during swing | 11.3 | 6.2 | 3.0 | 28.0 | 13.3 | 7.6 | 3.1 | 29.4 | 0.3 |
| Coronal hindfoot ROM throughout GC | 12.8 | 6.4 | 3.7 | 28.8 | 14.4 | 6.8 | 4.5 | 29.4 | 0.3 |
| Average coronal hindfoot position throughout GC | −15.5 | 11.0 | −42.1 | 11.7 | −2.1 | 12.0 | −31.1 | 12.7 | 1.2 |
| Coronal forefoot position at IC | 6.8 | 8.8 | −12.1 | 28.4 | 2.5 | 5.2 | −5.0 | 15.9 | 0.6 |

| Variables | CP | | | | Typically developing children | | | | Effect size |
|---|---|---|---|---|---|---|---|---|---|
| | Average | SD | Range | | Average | SD | Range | | |
| | | | Min | Max | | | Min | Max | |
| Peak forefoot valgus throughout GC | 11.5 | 9.3 | −9.7 | 32.7 | 6.4 | 4.4 | 0.7 | 18.6 | 0.7 |
| Peak forefoot varus throughout GC | −27.0 | 13.0 | −50.5 | −0.4 | −22.3 | 9.0 | −40.6 | −9.8 | 0.4 |
| Coronal forefoot ROM during stance | 34.6 | 16.2 | 2.4 | 62.9 | 26.7 | 11.4 | 4.6 | 54.1 | 0.6 |
| Coronal forefoot ROM during swing | 33.7 | 16.4 | 3.9 | 60.6 | 25.8 | 11.6 | 9.3 | 50.8 | 0.6 |
| Coronal forefoot ROM throughout GC | 38.6 | 16.7 | 3.9 | 65.3 | 28.7 | 11.7 | 10.5 | 56.8 | 0.7 |
| Average coronal forefoot position throughout GC | −2.9 | 6.7 | −19.9 | 6.6 | −3.8 | 3.8 | −12.5 | 2.5 | 0.2 |
| Transverse plane kinematics | | | | | | | | | |
| Transverse forefoot position at IC | −26.3 | 14.9 | −50.0 | 5.6 | −14.5 | 10.9 | −35.8 | 4.1 | 0.9 |
| Peak forefoot abduction throughout GC | −17.0 | 13.7 | −46.0 | 9.0 | −3.6 | 8.4 | −25.6 | 11.2 | 1.2 |
| Peak forefoot adduction throughout GC | −34.9 | 15.9 | −60.8 | −0.4 | −18.4 | 9.9 | −38.1 | 0.1 | 1.3 |
| Transverse forefoot ROM during stance | 15.8 | 9.6 | 4.9 | 54.3 | 12.0 | 5.0 | 7.3 | 26.0 | 0.5 |
| Transverse forefoot ROM during swing | 15.4 | 10.3 | 4.5 | 51.7 | 11.2 | 6.0 | 4.1 | 27.8 | 0.5 |
| Transverse forefoot ROM throughout GC | 17.9 | 6.4 | 6.5 | 29.1 | 14.1 | 5.1 | 8.3 | 27.8 | 0.7 |
| Average transverse forefoot position throughout GC | −26.2 | 14.4 | −49.5 | 4.8 | −11.4 | 9.5 | −31.4 | 6.5 | 1.2 |

## *3.1. Principal component analysis*

Of the 40 variables used in the first iteration of the PCA, 14 were removed from further analyses because they did not satisfy the retention criteria. The final dataset of 26 variables across 44 participants was determined to be suitable for PCA since a strong relationship among the variables was identified using Bartlett's test of sphericity ($p < 0.001$). Furthermore, there was adequate sampling as determined by the Kaiser–Meyer–Olkin test (KMO = 0.612). A KMO below 0.50 would be considered unacceptable to apply PCA.[26] The remaining 26 variables shown in Table 2 were ultimately reduced to six PCs (PC1–PC6) with eigenvalues ranging from 8.5 (PC1) to 1.5 (PC6). Weighting scores of the individual variables ranged from −0.70 to

−0.81 and 0.83 to 0.97. Additionally, the six retained PCs accounted for 92% of the cumulative variance of the dataset. Constructs of the PCs were then reviewed to provide a clinically relevant interpretation of the data taking into account the relationship among the variables within each of the six PCs (Table 3).

**Table 2.** Individual weighting scores and the amount of variance accounted for among variables within the retained principal components ($h^2$). The eigenvalues and cumulative variance are also reported for each principal component.

| Variable name | Principal component (eigenvalue, % cumulative variance) | | | | | | $h^2$ |
|---|---|---|---|---|---|---|---|
| | 1 (8.54, 32.8%) | 2 (6.7, 58.5%) | 3 (3.0, 70.1%) | 4 (2.5, 79.7%) | 5 (1.7, 86.3%) | 6 (1.5, 91.9%) | |
| Sagittal hindfoot position at IC | 0.94 | | | | | | 0.95 |
| Peak hindfoot dorsiflexion during stance | 0.96 | | | | | | 0.98 |
| Peak hindfoot plantarflexion during stance | 0.94 | | | | | | 0.99 |
| Peak hindfoot dorsiflexion during swing | 0.97 | | | | | | 0.98 |
| Peak hindfoot plantarflexion during swing | 0.93 | | | | | | 0.99 |
| Sagittal hindfoot ROM during stance phase | | | | | 0.94 | | 0.92 |
| Sagittal hindfoot ROM during swing phase | | | | | 0.87 | | 0.79 |
| Sagittal hindfoot ROM throughout GC | | | | | 0.94 | | 0.94 |
| Average sagittal hindfoot position during stance | 0.97 | | | | | | 0.98 |
| Average sagittal hindfoot position during swing | 0.97 | | | | | | 0.98 |
| Coronal hindfoot position at IC | | | 0.92 | | | | 0.92 |
| Peak hindfoot eversion throughout GC | | | 0.89 | | | | 0.98 |
| Peak hindfoot inversion throughout GC | | | 0.90 | | | | 0.98 |
| Coronal hindfoot ROM during stance | | | | 0.90 | | | 0.93 |
| Coronal hindfoot ROM during swing | | | | 0.92 | | | 0.96 |

| Variable name | Principal component (eigenvalue, % cumulative variance) | | | | | | $h^2$ |
|---|---|---|---|---|---|---|---|
| | 1 (8.54, 32.8%) | 2 (6.7, 58.5%) | 3 (3.0, 70.1%) | 4 (2.5, 79.7%) | 5 (1.7, 86.3%) | 6 (1.5, 91.9%) | |
| Coronal hindfoot ROM throughout GC | | | | 0.92 | | | 0.98 |
| Average coronal hindfoot position throughout GC | | | 0.94 | | | | 0.97 |
| Peak forefoot dorsiflexion throughout GC | −0.75 | | | | | | 0.79 |
| Coronal forefoot ROM during stance | | 0.93 | | | | | 0.96 |
| Coronal forefoot ROM during swing | | 0.93 | | | | | 0.59 |
| Coronal forefoot ROM throughout GC | | 0.91 | | | | | 0.95 |
| Average coronal forefoot position throughout GC | | | | | | −0.70 | 0.64 |
| Transverse forefoot position at IC | | −0.73 | | | | | 0.93 |
| Peak forefoot adduction throughout GC | | −0.81 | | | | | 0.95 |
| Transverse forefoot ROM during stance | | | | | | 0.83 | 0.71 |
| Transverse forefoot position throughout GC | | | | | | 0.90 | 0.96 |

**Table 3.** Constructs of the six principal components, number of participants assigned to each subgroup, interpretation of the subgroups, and the means (SE) of the individual principal component scores.

| Principal component (PC) | Construct | Principal component (PC) | Construct |
|---|---|---|---|
| PC1 | Sagittal hindfoot and forefoot equinus | PC4 | Coronal hindfoot varus excursion |
| PC2 | Transverse forefoot adduction and coronal forefoot excursion | PC5 | Sagittal hindfoot equinus escursion |
| PC3 | Coronal hindfoot varus | PC6 | Coronal forefoot varus and transverse forefoot excursion |

| Subgroup ($n$ = 44) | Description | PC1 | PC2 | PC3 | PC4 | PC5 | PC6 |
|---|---|---|---|---|---|---|---|
| #1 ($n$ = 18) | Control Group (rectus) | 114.3 (12.5) | 86.2 (9.5) | −1.2 (7.9) | 27.9 (2.1) | 41.7 (3.7) | 23.6 (1.8) |
| #2 ($n$ = 5) | Equinovarus deformity with primary hindfoot involvement | **−75.1 (24.5)**[*] | 77.0 (22.5) | **−65.0 (24.8)**[*] | 28.9 (8.4) | 58.9 (4.1) | 22.5 (3.3) |
| #3 ($n$ = 8) | Equinovarus deformity with | **−6.4 (23.2)**[*] | **182.3 (16.5)**[*] | **−67.8 (10.8)**[*] | 24.5 (3.7) | 32.6 (2.8) | 26.4 (3.1) |

| Principal component (PC) | Construct | | | | | |
|---|---|---|---|---|---|---|
| | hindfoot and forefoot involvement | | | | | |
| #4 (*n* = 8) | Varus deformity with both hindfoot and forefoot involvement (cavus) | 104.1 (33.7) | **172.5 (12.5)*** | **−61.3 (7.4)*** | **62.0 (5.4)*** | 47.4 (4.5) | 31.4 (4.3) |
| #5 (*n* = 5) | Forefoot adductus | 39.0 (15.7) | **164.7 (14.7)*** | −26.7 (20.8) | 32.6 (5.2) | 44.1 (5.9) | **54.0 (5.8)*** |

*Represents a significant difference from the Control Group (Subgroup #1) at $p < 0.05$.

## 3.2. Cluster analysis

Using the agglomeration schedule from the hierarchical cluster analysis, the first significant change in the distance coefficients was identified at stage 39. Subtracting 39 from the total number of subjects yielded five clusters (subgroups) for the *K*-means analysis. Fifteen of the 20 TD children and three children with CP were assigned to Subgroup #1 and was thus considered the Control Group. The remaining TD children were assigned to Subgroups #2 (*n* = 1) and #4 (*n* = 4). The ANOVA test identified an effect of subgroup membership for each of the PC scores. Post hoc testing identified each of the remaining four subgroups' unique characteristics of equinovarus when compared to the Control Group. Table 3 shows mean PC scores among the five subgroups:

- **Subgroup #1**: *Control Group:* Participants in Subgroup #1 included 15 TD children and three with CP.
- **Subgroup #2**: *equinovarus deformity with primary hindfoot involvement:* participants in Subgroup #2 (*n* = 3 children with CP and *n* = 1 TD child) demonstrated hindfoot and forefoot equinus (PC1; $p < 0.001$) and hindfoot varus (PC3; $p = 0.004$).
- **Subgroup #3**: *equinovarus deformity with hindfoot and forefoot involvement:* participants in Subgroup #3 (*n* = 8 children with CP) demonstrated similar hindfoot and forefoot equinus (PC1; $p = 0.001$) and hindfoot varus (PC3; $p < 0.001$) to individuals in Subgroup #2, as well as, additional forefoot adduction (PC2; $p < 0.001$). Individual PC Scores relative to those of the Control Group are presented in Fig. 1.
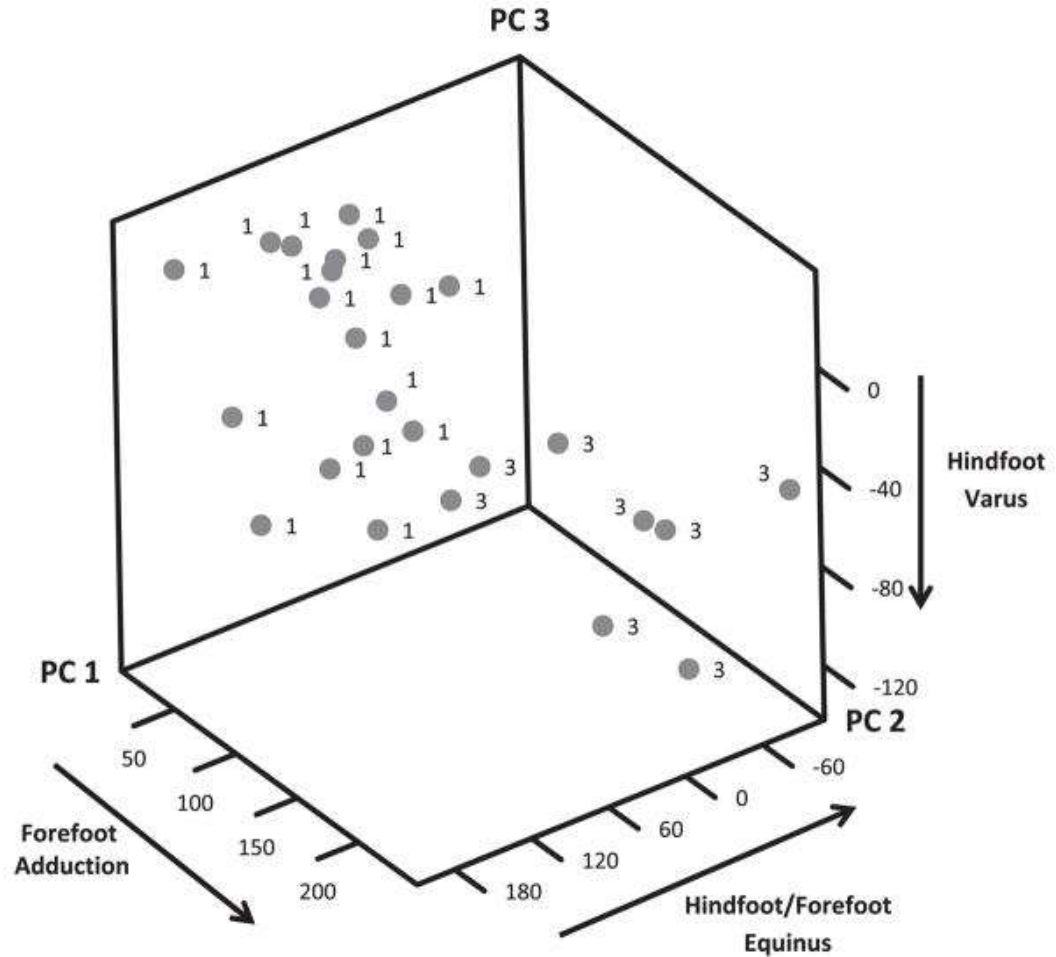
**Fig. 1.** Individual PC scores of the Control Group and Subgroup #3 for PC's 1 (sagittal hindfoot and forefoot equinus), 2 (transverse forefoot adduction and coronal forefoot flexibility), and 3 (coronal hindfoot varus). Participants in Subgroup #3 presented with equinus and varus hindfoot, as well as, an adducted forefoot relative to the Control Group.

- **Subgroup #4**: *varus deformity with hindfoot and forefoot involvement:* participants in Subgroup #4 ($n = 4$ children with CP and $n = 4$ TD children) demonstrated forefoot adduction (PC2; $p < 0.001$), hindfoot varus (PC3; $p = 0.001$), and increased, to the point of being excessive, coronal hindfoot ROM (PC4; $p < 0.001$) relative to the Control Group.
- **Subgroup #5**: *forefoot adductus:* participants in Subgroup #5 ($n = 5$ children with CP) demonstrated forefoot adduction (PC2; $p = 0.002$) and increased, excessive, transverse forefoot ROM (PC6; $p < 0.001$) relative to the Control Group.

The comparisons of PC scores between the Control Group and the other kinematic subgroups identified varying involvement of the different foot segments, in three planes, and varying ROM. Fig. 2(a)–(e) shows the mean segmental kinematics and one standard error of the Control Group along with the mean kinematics of each of the remaining four kinematic subgroups across the gait cycle. The observed deviations in segmental gait kinematics of the hindfoot and forefoot were consistent with the differences identified in the comparisons of the PC scores.
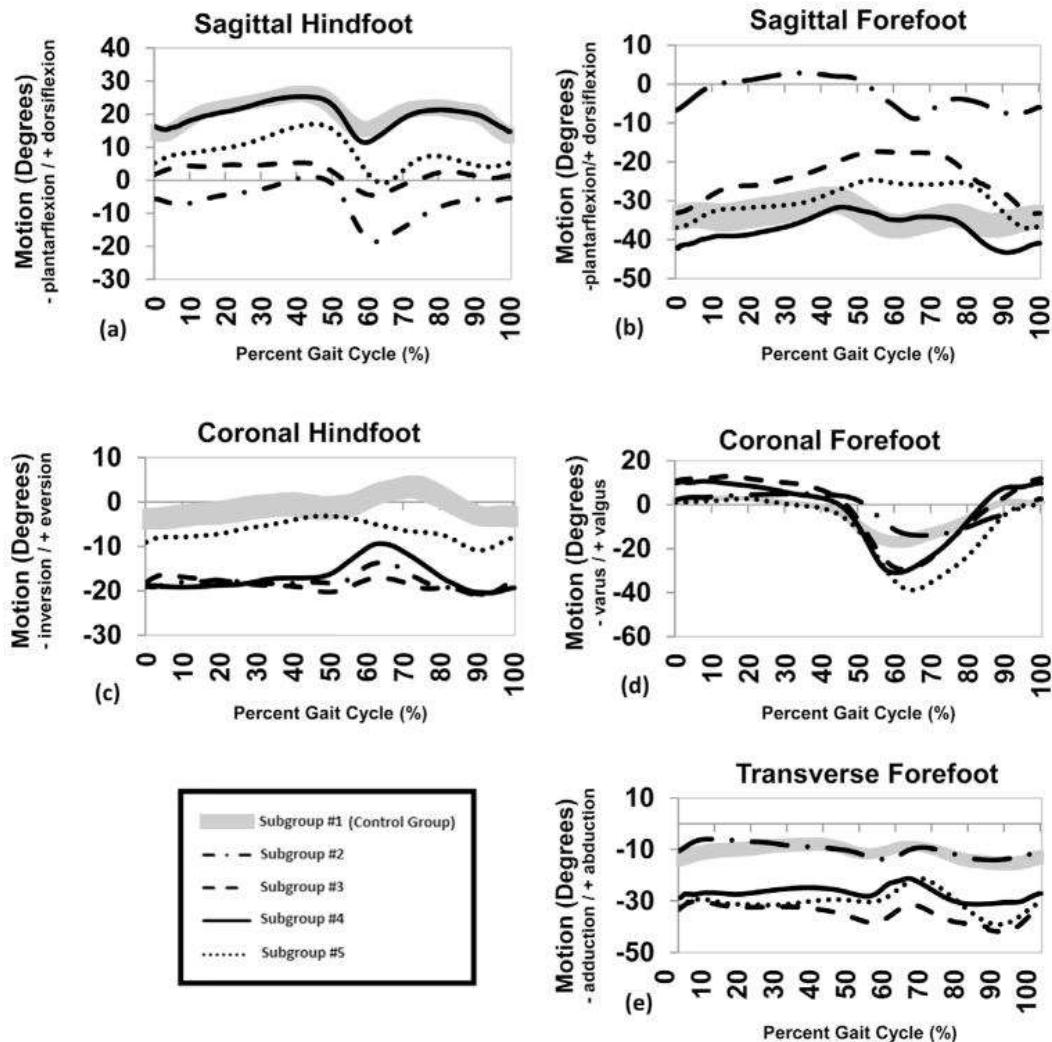


**Fig. 2.** Summary of mean sagittal hindfoot (a), sagittal forefoot (b), coronal hindfoot (c), coronal forefoot (d), and transverse forefoot (e) kinematics among Subgroups #2 through #4 and the mean with one standard error (gray band) for Subgroup #1 (Control Group).

# 4. Discussion

The current study identified five distinct, kinematic subgroups among a sample of TD children and children with equinovarus due to hemiplegic CP using 3-D multi-segment foot andanklekinematics as inputs for PCA and *K*-means cluster analysis. PCA reduced clinically relevant kinematic variables describing the location and plane of involvement in the foot and ankle to six PCs. Cluster analysis identified subgroups of participants with equinovarus who presented with variable involvement ranging from primary hindfoot or forefoot deviations to deformtiy that included the entire foot in multiple planes.

Although most of the TD children were assigned to Subgroup #1, they were not all clustered together. Fifteen were assigned to Subgroup #1, four to Subgroup #4, and one to Subgroup #2. This is explained by the inherent variability of healthy, asymptomatic, feet. Three biomechanical foot types have been identified in healthy adults: planus (low arched with valgus hindfoot and/or varus forefoot), rectus (well aligned hindfoot and forefoot), and cavus (high arched with a varus hindfoot and/or valgus forefoot).[29,30] In the current study, Subgroup #1 can be identified as having a rectus foot type with a well aligned hindfoot and forefoot. Subgroup #4 is consistent with a cavus foot type which includes hindfoot varus throughout the gait cycle, forefoot valgus during stance, increased peak forefoot varus at the end of stance phase, and forefoot adduction throughout the gait cycle (Table 3). In the current study, 4/20 (20%) of TD feet were identified as cavus which is consistent with previous research on larger samples of healthy adults.[29,31]

Subgroups #2–5 presented with kinematic characteristics consistent with previous literature which reported multiple types of equinovarus in children with CP.[5] This variability results from the combination of possible neuromuscular contributors affecting foot biomechanics. EMG studies demonstrated that varus deformity in children with hemiplegic CP resulted from the anterior tibialis alone in 34% of cases, posterior tibialis alone in 33%, both muscles in 31%, and muscles other than the anterior/posterior tibialis in 2%.[11] Additionally, the ankle plantar flexors, particularly the soleus, are potential contributors to equinovarus as they act as subtalar invertors

due to a medial insertion of the Achilles tendon on the calcaneus.[12] Thus, it is fitting that four distinct subgroups among a sample of children with equinovarus were identified in the present study when multi-segment kinematic analysis was performed.

Participants in Subgroups #2 and #3 presented with equinus (PC1) and hindfoot varus (PC3) (Table 3). However, participants in Subgroup #3 additionally exhibited forefoot involvement (PC2). The combination of equinus and hindfoot varus is consistent with involvement of the plantar flexors and/or the posterior tibialis.[12,32] Cadaveric studies identified that the posterior tibialis has the largest inversion moment arm across the subtalar joint and also acts as a plantar flexor of the talocrural joint.[32] Thus, treatment of the feet in Subgroups #2 and #3 should target the plantar flexors and the posterior tibialis to address the combination of equinus, hindfoot varus, and forefoot adduction. Participants in Subgroup #4 presented with hindfoot varus (PC3), but they did not have equinus (PC1) (Table 3). The lack of equinus can eliminate the involvement of the plantar flexors, and along with forefoot involvement (PC2), directs attention to the anterior tibialis. The anterior tibialis' insertion on the first metatarsal creates an inversion moment about the subtalar joint. Additionally, the anterior tibialis' insertion on the forefoot creates a dorsiflexion moment about the talocrural joint. This dorsiflexion moment arm is larger than the plantar flexion moment arm of the posterior tibialis.[32] Participants in Subgroups #3–5 each demonstrated coronal and transverse forefoot deviations, as well as, increased forefoot ROM (PC2 and PC6). Thus, the anterior tibialis most likely contributes to the deformity in these individuals, and surgery including a split transfer of the anterior tibialis to the cuboid may be indicated. However, since we did not include EMG analyses here, further validation of these predictive hypotheses is warranted.

A potential limitation in the current study was that the participants with CP specifically presented with unilateral equinovarus and a plan of possible surgical correction consisting of musculotendinous lengthenings and/or transfers. Therefore, generalization of these results to other patient populations commonly presenting with equinovarus deformity, such as diplegic cerebral palsy, talipes equinovarus, and Charcot–Marie–Tooth, should be cautioned. Another limitation was that even in an effort to create an objective

method for identifying subgroups of children with equinovarus, some level of subjective interpretation was still required. For example, to determine the a priori number of $K$ clusters, identification of the first significant change in distance coefficients following the hierarchical cluster analysis was required. This was performed by looking at a scree diagram of the agglomeration schedule produced by the hierarchical cluster analysis and choosing the point where the first significant change occurred. Regardless, highly significant differences were observed in the final comparisons of the PC scores among the clusters, findings were consistent with previous reports, and a clear clinical interpretation of the results was made. Finally, it should be recognized that when using these techniques with small sample sizes, non-reproducible findings can be a concern. A growing body of evidence using these techniques exists in the literature using samples as small as ten subjects.[15,33] These studies have demonstrated that systematic differences between the gait patterns of healthy and non-healthy individuals can be identified even in small-sized test groups after combining the data from both samples and using PCA as a mathematical tool that analyses the interrelation between variables.[33] In the current experiment we are optimistic about the reproducibility of our findings, and subsequent conclusions, because of significant mean differences identified between the CP and Control Groups when comparing the initial variables, the magnitude of the eigenvalues, the amount of cumulative variance accounted for by the PCs, the magnitude of the PC scores of the variables retained among the PCs, and the clear clinical interpretation of the findings. Ongoing work to provide further validation to these findings, including cross-validation techniques, is under way.

In summary, the current study presented an objective means to classify the multi-segment foot and ankle kinematics in children with equinovarus deformity secondary to hemiplegic CP and TD children. Five distinct kinematic subgroups were identified with involvement of the different foot segments, in different planes, and varying degrees of ROM when compared to a control group. These quantitative methods can ultimately be used to analyze severity and track progression of deformity. When used in conjunction with information such as kinetics, EMG, and physical examination measures, identification of segmental involvement utilizing kinematic subgroups would also facilitate treatment planning.

## Acknowledgments

## Footnotes

## Conflict of interest

No author of this paper has a conflict of interest, including specific financial interests, relationships, and/or affiliations relevant to the subject matter or materials included in this paper.

## References

[1] Wren TA, Rethlefsen S, Kay RM. Prevalence of specific gait abnormalities in children with cerebral palsy: influence of cerebral palsy subtype, age, and previous surgery. *J Pediatr Orthop*. 2005;25(1):79–83.

[2] Stebbins J, Harrington M, Thompson N, Zavatsky A, Theologis T. Gait compensations caused by foot deformity in cerebral palsy. *Gait Posture*. 2010;32(2):226–30.

[3] van den Hecke A, Malghem C, Renders A, Detrembleur C, Palumbo S, Lejeune TM. Mechanical work: energetic cost, and gait efficiency in children with cerebral palsy. *J Pediatr Orthop*. 2007;27(6):643–7.

[4] Ballaz L, Plamondon S, Lemay M. Ankle range of motion is key to gait efficiency in adolescents with cerebral palsy. *Clin Biomech (Bristol Avon)* 2010;25(9):944–8.

[5] Theologis T, Stebbins J. The use of gait analysis in the treatment of pediatric foot and ankle disorders. *Foot Ankle Clin*. 2010;15(2):365–82.

[6] Chang CH, Albarracin JP, Lipton GE, Miller F. Long-term follow-up of surgery for equinovarus foot deformity in children with cerebral palsy. *J Pediatr Orthop*. 2002;22(6):792–9.

[7] Scott AC, Scarborough N. The use of dynamic EMG in predicting the outcome of split posterior tibial tendon transfers in spastic hemiplegia. *J Pediatr Orthop*. 2006;26(6):777–80.

[8] Vogt JC. Split anterior tibial transfer for spastic equinovarus foot deformity: retrospective study of 73 operated feet. *J Foot Ankle Surg*. 1998;37(1):2–7. discussion 78.

[9] Barnes MJ, Herring JA. Combined split anterior tibial-tendon transfer and intramuscular lengthening of the posterior tibial tendon. Results in

patients who have a varus deformity of the foot due to spastic cerebral palsy. *J Bone Joint Surg Am*. 1991;73(5):734–8.

[10] Winters TF, Jr, Gage JR, Hicks R. Gait patterns in spastic hemiplegia in children and young adults. *J Bone Joint Surg Am*. 1987;69(3):437–41.

[11] Michlitsch MG, Rethlefsen SA, Kay RM. The contributions of anterior and posterior tibialis dysfunction to varus foot deformity in patients with cerebral palsy. *J Bone Joint Surg Am*. 2006;88(8):1764–8.

[12] Perry J, Burnfield JM. *Gait analysis: normal and pathological function*. 2. Thorofare NJ: SLACK Inc; 2010.

[13] Kidder SM, Abuzzahab FS, Harris GF, Johnson JE. A system for the analysis of foot and ankle kinematics during gait. *IEEE Trans Rehabil Eng.* 1996;4(1):25–32.

[14] Krzak JJ, Corcos DM, Graf A, Smith PA, Harris GF. Effect of fine wire electrode insertion on gait patterns in children with hemiplegic cerebral palsy. *Gait Posture*. 2013;37(2):251–7.

[15] Carriero A, Zavatsky A, Stebbins J, Theologis T, Shefelbine SJ. Determination of gait patterns in children with spastic diplegic cerebral palsy using principal components. Gait Posture. 2009;29(1):71–5.

[16] Shemmell J, Johansson J, Portra V, Gottlieb GL, Thomas JS, Corcos DM. Control of interjoint coordination during the swing phase of normal gait at different speeds. *J Neuroeng Rehabil*. 2007;4:10.

[17] Rozumalski A, Schwartz MH. Crouch gait patterns defined using *k*-means cluster analysis are related to underlying clinical pathology. *Gait Posture*. 2009;30(2):155–60.

[18] Johnson JE, Lamdan R, Granberry WF, Harris GF, Carrera GF. Hindfoot coronal alignment: a modified radiographic method. *Foot Ankle Int.* 1999;20(12):818–25.

[19] Cohen J. *Statistical power analysis for the behavioral sciences*. 2. Hillsdale, NJ: Erlbaum; 1988.

[20] Kaiser H. The application of eletronic computers to factor analysis. *Educ Phychol Meas*. 1960;20:141–51.

[21] Cattell R. The scree test for the number of factors. *Multivar Behav Res.* 1966;1(2):245–76.

[22] Jolliffe IT. *Principal component analysis*. 2. New York, NY: Springer; 2002.

[23] Kaiser HF. The application of electronic computers to factor analysis. *Educ Psychol Meas*. 1960;20:141–51.

[24] Stevens J. *Applied multivariate statistics for the social science*. NJ, USA: Hill Sdale; 1986.

[25] Bartlett MS. A not on the multiplying factors for various chi square approximations. *J Royal Stat Soc*. 1954;16:296–8.

[26] Kaiser HF. An index of factorial simplicity. *Psechometrika*. 1974;39:31–6.

[27] Ferrarin M, Bovi G, Rabuffetti M, Mazzoleni P, Montesano A, Pagliano E, et al. Gait pattern classification in children with Charcot–Marie–Tooth disease type 1A. *Gait Posture*. 2012;35(1):131–7.

[28] Ward JH. Hierarchical grouping to optimize an objective function. *J Am Stat Assoc.* 1963;48:236–44.

[29] Hillstrom HJ, Song J, Kraszewski AP, Hafer JF, Mootanah R, Dufour AB, et al. Foot type biomechanics part 1: structure and function of the asymptomatic foot. *Gait Posture*. 2012

[30] Mootanah R, Song J, Lenhoff MW, Hafer JF, Backus SI, Gagnon D, et al. Foot type biomechanics Part 2: are structure and anthropometrics related to function? *Gait Posture*. 2012

[31] Ledoux WR, Shofer JB, Smith DG, Sullivan K, Hayes SG, Assal M, et al. Relationship between foot type: foot deformity, and ulcer occurrence in the high-risk diabetic foot. *J Rehabil Res Dev*. 2005;42(5):665–72.

[32] Piazza SJ, Adamson RL, Sanders JO, Sharkey NA. Changes in muscle moment arms following split tendon transfer of tibialis anterior and tibialis posterior. *Gait Posture*. 2001;14(3):271–8.

[33] Federolf PA, Boyer KA, Andriacchi TP. Application of principal component analysis in clinical gait research: identification of systematic differences between healthy and medial knee-osteoarthritic gait. *J Biomech*. 2013;46(13):2173–8.

**Corresponding author at:** Midwestern University, Physical Therapy Program, College of Health Sciences, 555 31st Street, Downers Grove, IL, United States. Tel.: +1630 960-3942; fax: +1 630 515-7224. Email: joekkrzak@sbcglobal.net (J.J. Krzak)